Int J Adv Manuf Technol (2009) 45:33–40
DOI 10.1007/s00170-009-1932-z

ORIGINAL ARTICLE

Mathematical model of micro turning process

Iwona Piotrowska · Christina Brandt · Hamid Reza Karimi · Peter Maass

Received: 15 July 2008 / Accepted: 7 January 2009 / Published online: 29 January 2009

Abstract In recent years, significant advances in turning process have been achieved greatly due to the emergent technologies for precision machining. Turning operations are common in the automotive and aerospace industries where large metal workpieces are reduced to a fraction of their original weight when creating complex thin structures. The analysis of forces plays an important role in characterizing the cutting process, as the tool wear and surface texture, depending on the forces. In this paper, the objective is to show how our understanding of the micro turning process can be utilized to predict turning behavior such as the real feed rate and the real cutting depth, as well as the cutting and feed forces. The machine cutting processes are studied with a different model compared to that recently introduced for grinding process by Malkin and Guo (2006). The developed two-degrees-of-freedom model includes the effects of the process kinematics and tool edge serration. In this model, the input feed is changing because of current forces during the turning process, and the feed rate will be reduced by elastic deflection of the work tool in the opposite direction to the feed. Besides this, using the forces and material removal during turning, we calculate the effective cross-sectional area of cut to model material removal. With this model, it is possible for a machine operator, using the aforementioned turning process parameters, to obtain a cutting model at very small depths of cut. Finally, the simulated and experimental results prove that the developed mathematical model predicts the real position of the tool tip and the cutting and feed forces of the micro turning process accurately enough for design and implementation of a cutting strategy for a real task.

Keywords Turning process · Model analysis · Simulation

1 Introduction and notations

Turning is one of the most complex machining processes in manufacturing industry in which many variables can affect the desired results. With improvements in machine and spindle technology, an important and challenging issue in turning is the modeling of the process [9–11]. Recently, many papers that tackled the problem focused on dynamical representation of the turning processes, see, for instance, [1, 2] and the references therein. They present the dynamic modeling and simulation of the surface generation in turning process. In particular, they investigate the dynamic machining tool structural response, cutting process variables, tool geometry, and dynamic cutting force model. The force model plays an important role in material removal operation and has to be analyzed in detail. In [8], the authors present the dynamic cutting force model for the three-dimensional turning process. Moreover, different analytical stability models for turning

Ch. Brandt, H. R. Karimi and P. Maass were supported by the German Research Foundation DFG grant SPP 1180.
I. Piotrowska was supported by the German Research Foundation DFG grant SFB 747.

I. Piotrowska (✉)
Center of Industrial Mathematics, University of Bremen, 28359 Bremen, Germany
e-mail: iwona@math.uni-bremen.de

C. Brandt · H. R. Karimi · P. Maass
University of Bremen, Bremen, Germany

process models have been proposed in literature, see [5, 6] and [7]. Generally, these stability models consider the effects of important geometrical parameters such as the rake, inclination and side edge cutting angles and the insert tool radius.

In this paper, we present our recently developed concept of modelling of the micro turning process, i.e., a two-degrees-of-freedom (2DOF) model is developed for the actual feed rate of the tool. The starting point of this consideration is the development of a model for cutting and feed forces. The precise prediction of forces is very important for the effective simulation of the surface. Usually, the forces in cutting processes are modelled via Kienzle, see [3]. In this case, the force is proportional to the cross sectional area A, i.e.,

$$F = cA,$$

where c is a constant that takes the material parameters into account. This is the commonly used model that can be found in literature about cutting processes. Another approach for modelling of the forces is to assume that the force is given as the product of cross sectional area and velocity, i.e.,

$$F = cAv.$$

Thereby the model constant c has to be chosen correctly. This approach is proposed for grinding process in the references [14] and [16]. The experimental results show that the Kienzle approach is not effective for micro processes. For micro cutting processes, one has to consider a more general model that consists of the two aforementioned approaches:

$$F = c_1 A_1 + c_2 A_2 v. \tag{1}$$

We consider a single-point diamond micro plane turning process that provides a better understanding of the 2-dimensional turning dynamics and that considers the effects of important material and geometrical parameters. The impact of temperature on the process will remain unconsidered. We note that the rotational speed of the workpiece n is constant during the whole process. Thus, the cutting velocity is decreasing with time. This will impact on the course of the forces. In simulation results, the time behaviors of the model are shown and compared with measured results. Furthermore, effects of the rotational work speed, the machine stiffness in x- and y-directions, and disturbance on the feed velocity are studied separately. In general, it is shown that changes in the rotational work speed and depth of cut affect the noise during the turning process [12].

In the second step, the developed model has to be extended to a three-degrees-of-freedom model. The passive force model has to consist of two force terms because of a big influence of friction in this direction. This make the calculation more complicated and yields the numerical difficulties.

1.1 Notation

Now we collect the classical notions and well-known physical features that will be needed in the sequel. We will denote the time by t. The symbol K_e stands for the effective system stiffness. For a given feed f and the rotational work-speed n, the feed velocity is defined by

$$v_f = nf$$

and the workpiece velocity is

$$v_w = 2\pi nr.$$

It is assumed that the input depth of cut a_p and the feed rate f are smaller than the tool nose radius r_ε. Furthermore, we will use "a" writing top for actual variables depending on time.

f	The feed rate	ℓ_h	The length of the tool holder
v_f	The feed velocity	v_c	The cut velocity
a_p	The depth of cut	A_f	The cross-sectional area of feed
n	The rotational work-speed	A_c	The cross-sectional area of cut
r_ε	The tool radius	K_{ex}	The machine stiffness in x-direction
r	The workpiece radius	K_{ex}	The machine stiffness in y-direction
b_ε	The width of the tool in (Y,Z)-plane		

The rest of this paper is organized as follows. Section 2 includes the main results of the paper, that is, development of a 2DOF model for a turning process. Section 3 provides simulation results to illustrate and verify the specifications of the developed model for the process, and Section 4 concludes the paper.

2 Model description

In this section, a model is presented for the real position of the tool tip as well as the actual depth of cut. The basic idea is to investigate the forces that occur during the process. We remark that the model under

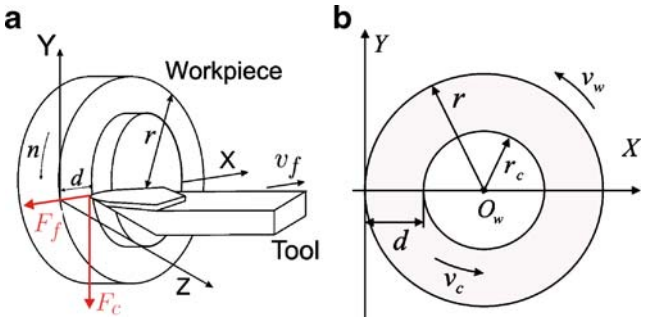

Fig. 1 Two-dimensional Cartesian coordinate system and forces in turning process (**a**, **b**)

consideration consists of two-dimensional case. More precisely, we include the two-dimensional model of the tool tip position as well as the force model for feed and cutting forces. We proceed to deal with the passive force and the actual position of the tool tip in the z-direction later on.

2.1 Process kinematics

In this subsection, we discuss in some detail on the geometry of the turning process. Recall that we consider the micro plane turning process with a single-point diamond tool restricted to orthogonal cutting. The cutting tool is moving along the radius to the center of the workpiece with a given feed rate f, see Fig. 1. In Fig. 2, one can see a two-dimensional image of the geometry and the movement of the turning tool on the workpiece surface. The geometry of the tool, vibrations, and the elastic deformations affect on the surface roughness. Note that the surface roughness in turning is also influenced by the depth of cut, the feed rate, the workpiece material, and its hardness. These elements determine the kinematic roughness. The interested reader is referred to [13] and [15] for further details.

For analyzing the forces, we will need the definition of the cross-sectional area. Recall that the cross-sectional area of cut A_c, see Fig. 2b, can be approximated by the product of the depth of cut a_p and the feed rate f, i.e., $A_c = a_p f$, see [13] and [15]. Similarly, the term $A_f = a_p b_\varepsilon$ is defined as the cross-sectional area of feed, see Fig. 2a. Moreover, for analyzing the dynamic forces, we will need the following dynamic definitions of the cross-sectional areas:

$$A_c(t) = f^a(t) a_p^a(t), \tag{2}$$

$$A_f(t) = b_\varepsilon a_p^a(t). \tag{3}$$

We will consider a general case and denote the friction area by $A_r(t)$. Note that the friction depends on the geometry of the workpiece. In our model, we take that $A(r)$ is modeled as step function. Moreover, we add the friction term only to the cutting force.

2.2 Force model

We start with considerations about the force model for the turning process. We confine attention to the feed force F_f and the cutting force F_c, see Fig. 1b. Neglecting the friction term in Eq. 1, the cutting force is given by

$$\begin{aligned} F_c(t) &= c_c A_c(t) v_c(t) + c_r A_r(t) \\ &= c_c 2\pi a_p^a(t) v_f^a(t)(r - d^a(t)) + c_r A_r(t), \end{aligned} \tag{4}$$

where c_c and c_r are model constants depending on materials. The displacement of the turning tool on the workpiece surface represented by $d^a(t)$ is computed as

$$d^a(t) = \int_0^t v_f^a(s)\mathrm{d}s = n \int_0^t f^a(s)\mathrm{d}s. \tag{5}$$

Furthermore, recall that the cutting velocity $v_c(t)$ is the rotational velocity with respect to the radius $r - d^a(t)$. The cutting force F_c affects the work tool and is responsible for its elastic deflection in the orthogonal direction to the feed. The feed force has the main influence on the elastic deflection of the work tool in the opposite direction to the feed. We define the feed force by

$$F_f(t) = c_f A_f(t) v_f^a(t) = c_f b_\varepsilon a_p^a(t) v_f^a(t), \tag{6}$$

Fig. 2 Geometry of the turning process (**a**, **b**)

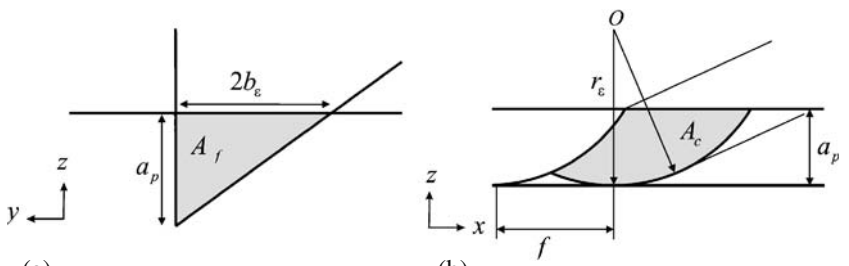

(a) The cross-sectional area in the plane orthogonal to the feed direction

(b) The cross-sectional area in the plane orthogonal to the cut direction

where c_f is a model constant. Both forces F_f and F_c depend on the time and affect the actual feed and the depth of cut.

2.3 Mathematical model

Our main task is the development of a 2DOF model that characterizes the displacement between command and actual position of the tool tip in micro turning processes. We take a similar approach to that in [16], which investigates the model for a cylindrical plunge grinding process. In this case, the actual infeed rate is reduced by the elastic deflection and the radial wear rate of the wheel. For more details, we refer the reader to [14]. Because of the diamond construction and the diameter of the cutting tool, the last effect does not occur in our turning process. We introduce the two-dimensional Cartesian coordinate system (X, Y) in such a way that the tool tip is at the origin at the beginning of the process, see Fig. 1a. The feed force F_f and the cutting force F_c affect on the tool and lead to the displacement at the X, and Y axes, respectively. We denote the deflections at the time t in x and y directions by $\delta_x(t)$ and $\delta_y(t)$, respectively. Then, the actual position P_s of the tool tip in the coordinate system (X, Y) is given by

$$P_{s,x}(t) = v_f\, t - \delta_x(t)\,, \tag{7}$$

$$P_{s,y}(t) = -\delta_y(t)\,. \tag{8}$$

A careful look at Eq. 5 reveals that $d^a(t) = P_{s,x}(t)$. Moreover, by taking the derivative of Eq. 7 and together with Eq. 5, we obtain

$$v_f^a(t) = v_f - \dot{\delta}_x(t). \tag{9}$$

It is clear that the actual feed velocity depends on the given feed velocity and the derivative of the displacement of the tool tip $\dot{\delta}_x(t)$. The deflection is computed as usual, i.e., the appropriate force F over the process stiffness K_e. In our model, we distinguish two machine stiffnesses for two directions, i.e., K_{ex} and K_{ey}, which

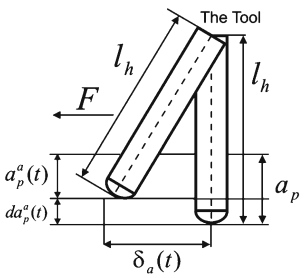

Fig. 3 The actual depth of cut

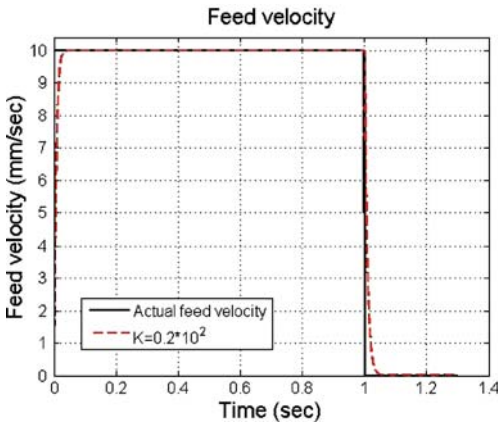

Fig. 4 Curves of the feed rate velocity and the actual feed rate velocity signals

depend on height, width, and length of the tool holder, as well as on the material properties. Thus, we have

$$\frac{F_f(t)}{K_{ex}} \qquad \text{and} \qquad \frac{F_c(t)}{K_{ey}}.$$

This, in conjunction with Eq. 6, yields the formula of the deflection in the x direction

$$\delta_x(t) = \frac{F_f(t)}{K_{ex}} = \frac{c_f b_\varepsilon}{K_{ex}} a_p^a(t) v_f^a(t). \tag{10}$$

For the deflection in the y direction, we combine Eq. 4 with the relation Eq. 5 and obtain

$$\delta_y(t) = \frac{F_c(t)}{K_{ey}} = \frac{c_c 2\pi}{K_{ey}} a_p^a(t) v_f^a(t) \left(r - \int_0^t v_f^a(s)\mathrm{d}s\right) + c_r A_r(t). \tag{11}$$

We simplify the writing by denoting two constants c_x and c_y in Eqs. 10 and 11 as $c_x = \frac{c_f b_\varepsilon}{K_{ex}}$ and $c_y = \frac{c_c 2\pi}{K_{ey}}$, respectively. Further, we distinguish the active force F_a,

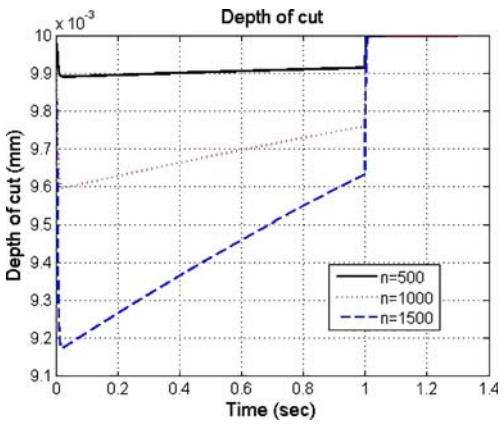

Fig. 5 Time histories of the actual depth of cut

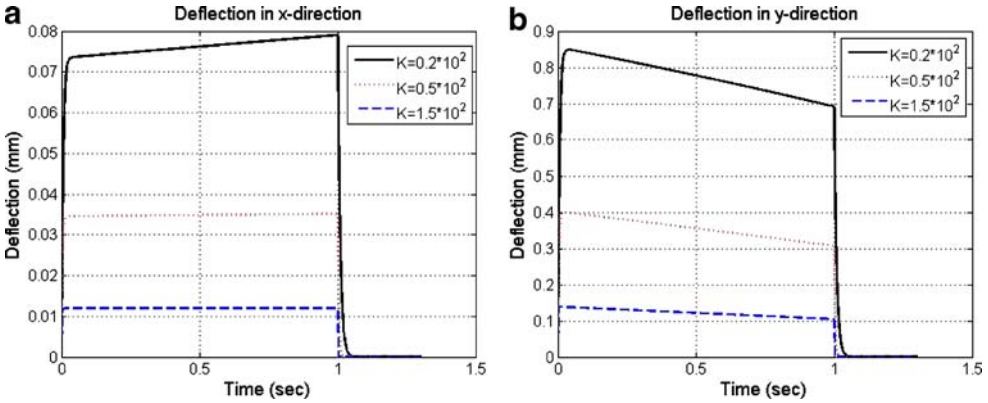

Fig. 6 Curves of deflections in both x and y directions (**a**, **b**)

which is defined as the sum of F_f and F_c, i.e., $F_a = F_f + F_c$, see Fig. 1. This affects the tool and determines the total displacement of the tool δ_a, which is given by

$$\delta_a(t) = \sqrt{\delta_x(t)^2 + \delta_y(t)^2}\,.$$

Figure 3 shows the displacement in the depth of cut da_p^a, which is also effected by the total tool displacement δ_a. By the Pythagoras theorem, we obtain

$$da_p(t) = l_h - \sqrt{l_h^2 - \delta_a(t)^2} \approx l_h - \left(l_h - \frac{\delta_a(t)^2}{2l_h}\right) = \frac{\delta_a(t)^2}{2l_h}\,,$$

where l_h denotes the length of the tool holder. The last term is obtained by taking into account the two first positions from Taylor series expansion of the root. Then, the actual depth of cut can be obtained with the following expression:

$$a_p^a(t) \approx a_p - \frac{\delta^a(t)^2}{2\ell_h}. \tag{12}$$

Now, we are in a position to define the differential equations system. The first equation for the deflection in the x direction has already been given by Eq. 9. For the deflection in the y direction, we put Eq. 10 in Eq. 11 and get

$$\delta_y(t) = \frac{c_y}{c_x}\delta_x(t)\left(r - \int_0^t v_f^a(\tau)\,\mathrm{d}\tau\right) + c_r A_r(t).$$

The derivative yields

$$\dot{\delta}_y(t) = \frac{c_y}{c_x}\left[\dot{\delta}_x(t)\left(r - \int_0^t v_f^a(\tau)\,\mathrm{d}\tau\right) - \delta_x(t)v_f^a(t)\right] + c_r\dot{A}_r(t).$$

Furthermore, we put Eq. 9 into the above equation and obtain

$$\dot{\delta}_y(t) = \frac{c_y}{c_x}\left[\left(v_f - v_f^a(t)\right)\left(r - \int_0^t v_f^a(\tau)\,\mathrm{d}\tau\right) - \delta_x(t)v_f^a(t)\right] + c_r\dot{A}_r(t). \tag{13}$$

Now, we are interested in describing the equation for the actual depth of cut. The derivative of (12) is given by

$$\dot{a}_p^a(t) = -\frac{1}{l_h}\delta_a(t)\dot{\delta}_a(t)\,,$$

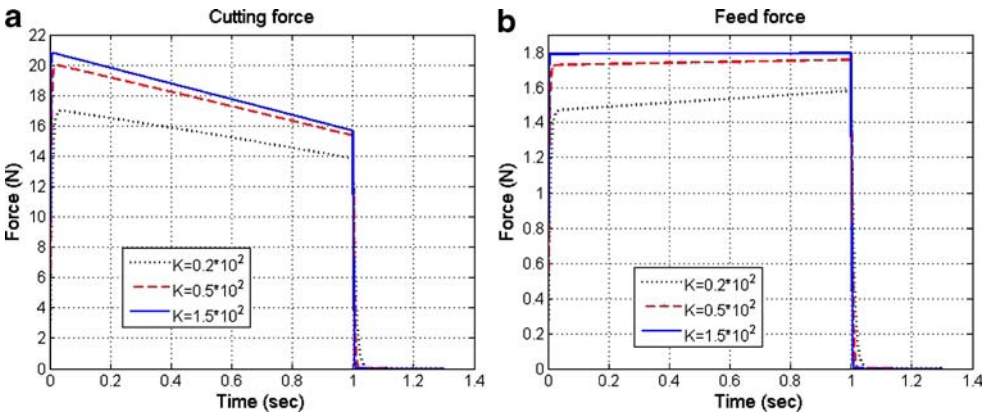

Fig. 7 Curves of the cutting and feed force (**a**, **b**)

Fig. 8 Ultra-precision single-point diamond turning machine

where

$$\dot{\delta}_a(t) = \frac{\delta_x(t)\dot{\delta}_x(t) + \delta_y(t)\dot{\delta}_y(t)}{\sqrt{\delta_x(t)^2 + \delta_y(t)^2}}.$$

After plugging Eqs. 9 and 13 into the above formula, we conclude

$$\begin{aligned}\dot{a}_p^a(t) &= -\frac{1}{l_h}\left(\delta_x(t)\dot{\delta}_x(t) + \delta_y(t)\dot{\delta}_y(t)\right)\\ &= -\frac{1}{l_h}\Bigg(\delta_x(t)\left(v_f - v_f^a(t)\right)\\ &\quad +\delta_y(t)\frac{c_y}{c_x}\left[\left(v_f - v_f^a(t)\right)\left(r - \int_0^t v_f^a(\tau)\,\mathrm{d}\tau\right)\right.\\ &\quad \left.-\delta_x(t)v_f^a(t)\right] + c_r\dot{A}_r(t)\Bigg). \end{aligned} \tag{14}$$

Then, Eq. 9 combined with $\dot{\delta}_x(t)$ and solved with respect to $\dot{v}_f^a(t)$ gives

$$\dot{v}_f^a(t) = \frac{v_f - \left(1 + c_x\dot{a}_p^a(t)\right)v_f^a(t)}{c_x a_p^a(t)}. \tag{15}$$

Finally, we have that

$$\dot{d}^a(t) = v_f^a(t). \tag{16}$$

Plugging Eq. 14 into Eq. 15 yields the last differential equation so that we obtain the following equation system:

$$\begin{cases} \dot{d}^a(t) = v_f^a(t), \\ \dot{v}_f^a(t) = \dfrac{v_f - \left(1 + c_x\dot{a}_p^a(t)\right)v_f^a(t)}{c_x a_p^a(t)}, \\ \dot{a}_p^a(t) = -\dfrac{1}{l_h}\Bigg(\delta_x(t)\left(v_f - v_f^a(t)\right) \\ \qquad +\delta_y(t)\dfrac{c_y}{c_x}\left[\left(v_f - v_f^a(t)\right)\left(r - \int_0^t v_f^a(\tau)\,\mathrm{d}\tau\right)\right. \\ \qquad \left.-\delta_x(t)v_f^a(t)\right] + c_r\dot{A}_r(t)\Bigg), \\ \dot{\delta}_x(t) = v_f - v_f^a(t), \\ \dot{\delta}_y(t) = \dfrac{c_y}{c_x}\left[\left(v_f - v_f^a(t)\right)\left(r - \int_0^t v_f^a(\tau)\,\mathrm{d}\tau\right) - \delta_x(t)v_f^a(t)\right]. \end{cases} \tag{17}$$

Remark 2.1 The feed velocity $v_f^a(t)$ and actual depth of cut $a_p^a(t)$ are calculated by solving the nonlinear differential equations Eq. 17 and considering the boundary conditions $d^a(0) = 0$, $v_f^a(0) = 0$, $a_p^a(0) = a_p$, and $\delta_x(0) = \delta_y(0) = 0$. Moreover, we can predict the feed and cutting forces using Eqs. 4 and 6, respectively, as well as the actual feed $f^a(t)$.

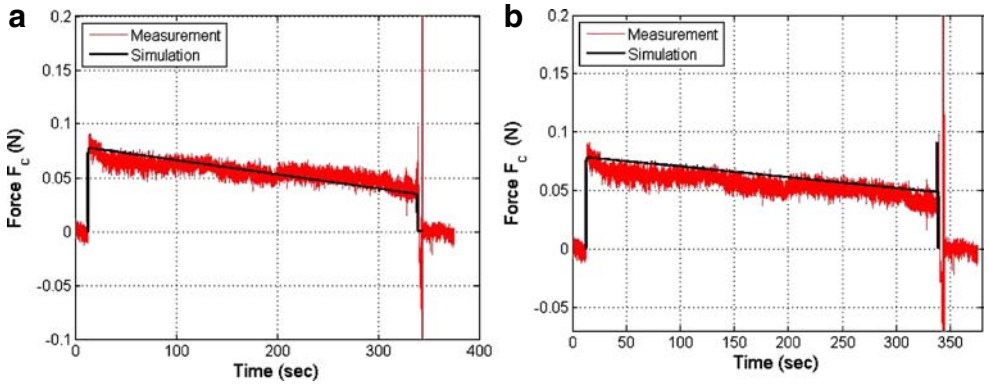

Fig. 9 Compression of measured and predicted cutting force (**a**, **b**)

Table 1 Experimental turning conditions

Test	Rotational velocity [min^{-1}]	Feed velocity $\frac{\text{mm}}{\text{min}}$	Depth of cut
Test 1	1000	5.51	5
Test 2	800	5.51	5

3 Simulated results and discussion

For simulation of the feed and the nonlinear equations system (Eq. 17), the MATLAB software takes two-stage input information, the workpiece properties, tool specification, and the process parameters. The developed model in Eq. 17 is then executed to predict turning behavior including feed rate, depth of cut, forces, and deflections.

3.1 Analysis of cutting and feed forces

The nonlinear differential equations of the system Eq. 17 have been solved numerically for the nominal system parameters: $K = K_{ex} = K_{ey} = 0.5 \cdot 10^2 \left[\frac{\text{N}}{\text{mm}}\right]$, $r = 40[\text{mm}]$, $b_\varepsilon = 0.2[\text{mm}]$, $\ell_h = 200[\text{mm}]$, $f = 0.01[\text{mm}]$, $n = 1000\left[\frac{\text{rev}}{\text{sec}}\right]$.

To illustrate the simulation, consider the two-stage feed rate as input shown in Fig. 4 together with the predicted actual feed rate f^a for the actual turning process in three different values of machine stiffness: $K = 0.2 \cdot 10^2, 0.5 \cdot 10^2, 1.5 \cdot 10^2 \left[\frac{\text{N}}{\text{mm}}\right]$. In Fig. 5, we show the time history of the actual depth of cut $a_p^a(t)$ for various rotational work-speeds: $n = 500,\ 1{,}000,\ 1{,}500\left[\frac{\text{rev}}{\text{s}}\right]$. Note that this case corresponds to a relatively small workpiece velocity. One can see that the cutting process is very smooth with small fluctuations around the assumed cutting depth. Figure 6 shows the deflections in the x and y directions, respectively, for three different values of the machine stiffness. It is seen that, during the process, the deflection in the y direction, i.e., $\delta_y(t)$, decreases, whereas $\delta_x(t)$ increases. Moreover, the curves of the feed force and cutting force are depicted in Fig. 7, also for three different values of the machine stiffness.

From Eqs. 10 and 11, we see that forces are proportional to the deflections, so we can observe the same effects like those in Fig. 6a and b.

3.2 Experimental results

This part illustrates the verification of the developed mathematical model for a turning process. The machine used in the experiments is the ultra precision single-point diamond turning machine, shown in Fig. 8. The verification of the model is effected for the cutting force. The force in the feed direction occurs during the process is relative small, which makes complications with the measurements. Therefore, we omit it in our consideration. Furthermore, the whole model, i.e., including the passive force, will be verified by comparing the surface characteristic parameters, like, for example, roughness.

In Fig. 9, close correspondence between the experimental and the simulated plots in Matlab for two different process records shown in Table 1 indicates that the developed model is accurate enough to analyze and predict the tool tip position for turning process.

3.3 Effect of external disturbances

Generally speaking, noise is a consequence of each cutting process and depends on the vibrations of the workpiece and machine tool. Vibrations of the surroundings (floor, other machine tools, and so on) represent disturbances in terms of tool wear monitoring [4].

For simulation purposes, a uniformly distributed random signal as the disturbance is imposed on the feed velocity. Therefore, the effect of external disturbances on the turning behavior including depth of cut is depicted for three different rotational work speeds in Fig. 10. Similarly, Fig. 11 shows three different curves of the depth of cut obtained under the same cutting conditions but with different machine stiffnesses $K = 0.2 \cdot 10^2,\ 0.5 \cdot 10^2,\ 1.5 \cdot 10^2 \left[\frac{\text{N}}{\text{mm}}\right]$ for the rotational work speed $n = 1{,}000\left[\frac{\text{rev}}{\text{s}}\right]$. The simulation results show that the process preserves the stability until a disturbance with minimum and maximum -0.001 and 0.001,

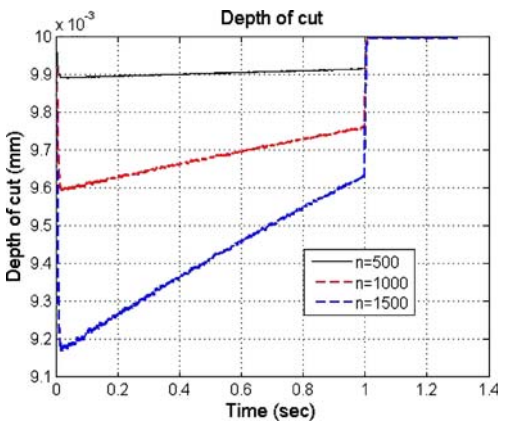

Fig. 10 Curves of the actual depth of cut in the presence of disturbance

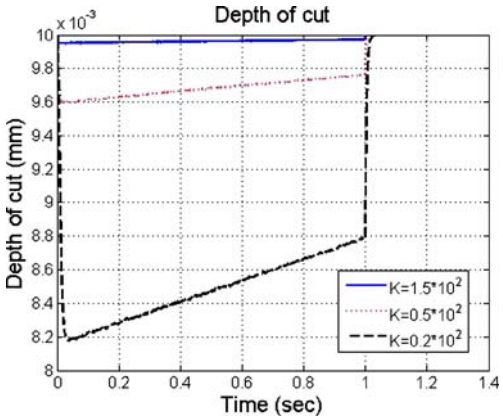

Fig. 11 Curves of the actual depth of cut in the presence of disturbance

respectively, and can be compared with the results without disturbance in Fig. 5. Furthermore, comparing the curves obtained for each of the depth of cut signals in Figs. 10 and 11, one notes that the signals are more influenced by the disturbance when machining under the same condition but for high rotational work speed or low machine stiffness. Nevertheless, it is important to note that the robust stability analysis of the obtained model in the presence of disturbances and uncertainties are still under investigation by the authors.

4 Conclusion

We have developed a novel 2DOF model for the micro turning processes to show how knowledge of the effects of the process kinematics and tool edge serration can be utilized to simulate the tool-workpiece system behavior. In this model, the input feed is changing because of current forces during turning process and the feed rate will be reduced by elastic deflection of the tool in opposite direction. It was shown that the model predicts the real position of the tool tip as well as the cutting and feed forces. Moreover, using the forces and material removal during turning, we calculated the effective cross-sectional area of cut to model material removal. One advantage of this model is that it makes possible for a machine operator to obtain a cutting model at very small depths of cut using the aforementioned turning process parameters. The 2DOF model of the turning process developed and verified in the paper can be extended to provide a better understanding on the multidimensional turning dynamics where the multidimensional modelling must be used for accurate predictions of the forces, the depth of cut, and the surface of the final product. Therefore, this extension is a topic currently under study.

References

1. Cheng K, Luo X, Ward R (2005) The effects of machining process variables and tooling characterisation on the surface generation. Int J Manuf Sci Technol 25:1089–1097
2. Cheng K, Luo XC, Luo XK, Liu XW (2005) A simulated investigatin on the machining instability and dynamic surface generation. Int J Manuf Sci Technol 26:718–725
3. Dassanayake AV, Suh CS (2008) On nonlinear cutting response and tool chatter in turning operation. Commun Nonlinear Sci Numer Simul 13:979–1001
4. Kopac J, Sali S (2001) Tool wear monitoring during the turning process. J Mater Process Technol 112:312–316
5. Olgac N, Zhao G (1987) A relative stability study on the dynamics of the turning mechanism. Trans ASME 109: 164–170
6. Ozlu E, Budak E (2006) Analytical stability models for turning and boring operations - part I: model development. ASME J Manuf Sci Eng 129(4):726–732
7. Ozlu E, Budak E (2007) Comparison of one-dimensional and multi-dimensional models in stability analysis of turning operations. Int J Mach Tools Manuf 47:1875–1883
8. Rao BC, Shin YC (1999) A comprehensive dynamic cutting force model for chatter prediction in turning. Int J Mach Tools Manuf 39:1631–1654
9. Ravindra HV, Srinivasa YG, Krishnamurthy R (1993) Modeling of tool wear based on cutting forces in turning. Wear 169(1):25–32
10. Wang J (2001) Development of a chip flow for turning operations. Int J Mach Tools Manuf 41:1265–1274
11. Wang J, Mathew P (1995) Development of a general tool model for turning operations based on a variable flow stress theory. Int J Mach Tools Manuf 35:71–90
12. Weller EJ, Schrier HM, Weichbrodt B (1969) What sound can be expected from a worn tool? J Eng Ind 91:525–534
13. Altintas Y (2000) Manufacturing automation: metal cutting mechanics. Machine tool vibrations and CNC design. Cambridge University Press, Cambridge
14. Malkin S (1989) Grinding technology: theory and application of machining with abrasives. Ellis Horwod and Wiley, Chichester (1996) (Reprinted by SME)
15. Riemer O (2001) Trennmechanismen und Oberflächenfeingestalt bei der Mirozerspannung kristallier und amorpher Werkstoffe. Aachen, Shaker
16. Malkin S, Guo C (2006) Model based simulation of grinding processes. http://www.abrasivesmagazine.com/mtext/product/Model%20Based%20Simulation.pdf